Pharmacological Evaluation and Computational Insights into Two Pyrazole Derivatives of (*E*)-3-(4-chlorophenyl)-1-phenylprop-2-en-1-one

K. M. Ferdousul Haque, Md. Khalid Hossain, Mohammad A. Rashid and Mohammad Sharifur Rahman

Department of Pharmaceutical Chemistry, Faculty of Pharmacy, University of Dhaka, Dhaka-1000, Bangladesh

(Received: August 15, 2025; Accepted: December 04, 2025; Published (web): December 25, 2025)

ABSTRACT: On a global scale, cancer and oxidative stress remain major health challenges**.** One such class of compounds is chalcones**,** which are 1,3-diaryl ketones containing an *α, β*-unsaturated carbonyl system. These ketones serve as precursors to numerous biologically active heterocyclic frameworks, including pyrazoles. In the present study, a chloro-chalcone, (*E*)-3-(4-chlorophenyl)-1-phenylprop-2-en-1-one (1), was prepared by condensing 4-chlorobenzaldehyde with acetophenone. It was then converted into two pyrazole derivatives, 5-(4-chlorophenyl)-3-phenyl-4,5-dihydro-1*H*-pyrazole (2) and 1-(5-(4-chlorophenyl)-3-phenyl-4,5-dihydropyrazol-1-yl) ethanone (3), via reaction with hydrazine hydrate followed by acetylation with acetic acid, respectively. The structures were confirmed using FT-IR and ^{1}H NMR spectroscopic analyses. When tested against HeLa cancer cells, all three compounds exhibited strong cytotoxic activity**,** reducing cell viability to below 5%**.** The antioxidant assays, which measured total antioxidant capacity and free radical scavenging, showed that compounds 1 through 3 had noticeable activity. Molecular docking predicted that compounds 1-3 formed strong binding interactions at the adenosine triphosphate binding site of the epidermal growth factor receptor protein (EGFR; PDB: 1M17). Compounds 1 and 2 may interact with CYP enzymes, whereas others demonstrated good oral absorption and blood-brain barrier permeability, according to Swiss ADME predictions. To the best of our knowledge, the biological and computational assays for these compounds have been conducted for the first time. Overall, the chalcone-pyrazole derivatives exhibited promising antioxidant and anticancer potential, warranting further biological and pharmacokinetic investigations.

Key words: *Para*-chlorochalcone, anticancer, pyrazole; antioxidant, HeLa cell.

INTRODUCTION

Chalcones have attracted considerable interest in medicinal chemistry because of their wide range of pharmacological properties. Structurally, they are characterized by two aromatic rings linked through an *α, β*-unsaturated carbonyl system. Studies have demonstrated that chalcones exhibit diverse biological activities, including antioxidant, antimicrobial, anticancer, antimalarial and anti-inflammatory effects, which make them valuable scaffolds for new drug development.[1] Structural modification—particularly through the introduction of heteroatoms such as chlorine, oxygen, or sulfur—has been shown to enhance their biological activity by improving potency and selectivity.[2,3] Among the various heterocyclic systems derived from chalcones, pyrazoles and their analogues have attracted particular attention because of their notable medicinal importance. These compounds display a broad spectrum of pharmacological effects, including antitubercular, anticonvulsant, analgesic, anti-inflammatory, anticancer, antidepressant, antipyretic, antibacterial and antioxidant activities. Their structural flexibility and pharmacophoric characteristics enable interactions with multiple molecular targets, making pyrazoles highly valuable in both pharmaceutical and agrochemical research.[4]

Correspondence to: Mohammad Sharifur Rahman
E-mail address: msr@du.ac.bd

Dhaka Univ. J. Pharm. Sci. **24**(2): 219-229, 2025 (December)
DOI: https://doi.org/10.3329/dujps.v24i2.86374

Cancer continues to pose a major global health challenge, affecting millions of people each year. Despite the availability of several chemotherapeutic agents, their clinical utility is often constrained by severe side effects, drug resistance and high treatment costs.[5] Consequently, there is a pressing need to discover new chemical entities capable of selectively targeting cancer cells. Pyrazole derivatives have emerged as promising anticancer candidates owing to their ability to modulate several key pathways, such as apoptosis induction, kinase inhibition, and cell cycle regulation.[6] Oxidative stress is a critical factor implicated in numerous chronic and degenerative diseases, including aging, diabetes, cardiovascular disorders, neurodegenerative conditions and cancer, where an imbalance between reactive oxygen species and antioxidant defenses contributes to cellular damage and tumor progression.[7,8] Oxidative stress arises from the excessive production of reactive oxygen species (ROS), which cause cellular injury through lipid peroxidation, protein oxidation, and DNA fragmentation, ultimately compromising the body's defense systems.[9] For this reason, the identification of potent antioxidant agents remains a central focus of drug discovery. Pyrazole-based compounds have demonstrated significant antioxidant potential owing to their ability to neutralize free radicals, chelate metal ions and modulate antioxidant enzymes.[10,11]

In the present work, a chloro-substituted chalcone, (*E*)-3-(4-chlorophenyl)-1-phenylprop-2-en-1-one (1), was synthesized *via* Claisen-Schmidt condensation of acetophenone with p-chlorobenzaldehyde. Two pyrazole derivatives were subsequently obtained: 5-(4-chlorophenyl)-3-phenyl-4, 5-dihydro-1*H*-pyrazole (2), produced by treatment with hydrazine hydrate and 1-(5-(4-chlorophenyl)-3-phenyl-4,5-dihydropyrazol-1-yl) ethanone (3), prepared through acetylation of compound 2 using acetic acid. The biological activities of these compounds were evaluated through antiproliferative assays against HeLa cervical cancer cells and antioxidant assays, including DPPH free radical scavenging and total antioxidant capacity measurements.

This dual investigation provided insight into both anticancer and antioxidant potential.[12] Molecular docking studies further revealed strong binding affinities of compounds 1-3 at the ATP-binding site of the epidermal growth factor receptor (EGFR) protein.[13,14] *In silico* ADME profiling using SwissADME also indicated favorable drug-likeness and pharmacokinetic characteristics.[15] To our knowledge, this is the first report presenting both biological and computational evaluations of these compounds. Overall, these findings offer a mechanistic explanation for the observed biological activities and provide a foundation for the rational design of new chalcone-pyrazole derivatives with enhanced therapeutic potential. The combined cytotoxic, antioxidant and EGFR-targeted properties of these compounds underscore their promise as lead structures for future drug development.[16]

MATERIALS AND METHODS

General experimental design and analytical instrumentation: The uncorrected melting points of all synthesized compounds were determined using a Gallenkamp apparatus (England). UV-visible spectra were recorded on a Shimadzu spectrophotometer in dry ethanol to analyze electronic transitions, while Fourier-transform infrared (FTIR) spectra were obtained to identify characteristic functional groups. ^{1}H NMR spectra were acquired using a Bruker spectrometer operating at 400 and 600 MHz. Reaction progress and compound purity were monitored at regular intervals by thin-layer chromatography (TLC) on pre-coated silica gel 60 F_{254} plates (purchased from E. Merck). Further purification of the crude products was achieved through column chromatography on silica gel (60-120 mesh) as the stationary phase. All chemicals and solvents used were of analytical grade and procured from reputable suppliers, including Merck (Germany) and Indian Loba Chemie (India).

Preparation of (*E*)-3-(4-chlorophenyl)-1-phenylprop-2-en-1-one (1). Acetophenone (0.60 g, 0.005 mol) and 4-chlorobenzaldehyde (0.70 g, 0.005 mol) were dissolved in ethanol and stirred with 45%

aqueous NaOH for 1 h at room temperature. The reaction mixture was then refrigerated for 24 h to allow the product to precipitate. The solid formed was filtered, recrystallized from ethanol and dried to yield the desired chalcone. The compound was characterized by melting point determination, UV, IR and ^{1}H NMR analyses.[17-19]

Yield 85%; Appearance: Yellowish solid; mp. 110-115°C; (IR (cm^{-1}): 3058 (C=C–H stretching, alkenyl), 1658 (C=O stretching, conjugated carbonyl), 1589 (C=C stretching, alkenyl), 1565 and 1486 (C=C stretching, aromatic ring), 1402–1446 (C–C stretching, aliphatic), 1214 (C–C/C–H in-plane bending, aromatic), 819 (C–Cl stretching). ^{1}H NMR (600 MHz, $CDCl_3$): δ 7.39 (2H, m, J = 7.8 Hz, H-6, H-8), 7.50 (3H, m, J = 6 Hz, H-2, H-11, H-13), 7.57 (3H, m, H-5, H-9, H-12), 7.76 (1H, d, J = 15.6 Hz, H-3), 8.01 (2H, m, H-10, H-14).

Preparation of 5-(4-chlorophenyl)-3-phenyl-4, 5-dihydro-1*H*-pyrazole (2). Compound 1 (1.21 g, mol) and hydrazine hydrate (0.25 g, 0.25 ml, 0.005 mol) were dissolved in 60 ml of ethanol. The reaction mixture was refluxed at 60-65°C for 15 h, and the progress of the reaction was monitored at regular intervals by thin-layer chromatography (TLC). Upon completion, the mixture was cooled in an ice–water bath to induce precipitation. The resulting solid was filtered and recrystallized from ethanol to afford the pure pyrazole derivative. The purified compound was dried under reduced pressure and characterized by melting point determination, UV–visible, FTIR and ^{1}H NMR analyses.[20,21]

Yield: 63%; Appearance: Light orange solid; mp: 128-131°C. IR (cm^{-1}): 3064 (C–H stretching, aromatic), 1589 (C=N stretching, imine), 1107 (C–N stretching, aliphatic), 824 (C–Cl stretching). ^{1}H NMR (600 MHz, $CDCl_3$): δ 3.06 (1H, m, H-4a), 3.35 (1H, m, H-4b), 5.31 (1H, m, J_1 = 4.8 Hz, J_2 = 3.6 Hz, H-5), 7.08 (1H, br s, NH-1), 7.20-7.60 (9H, m, Ar–H).

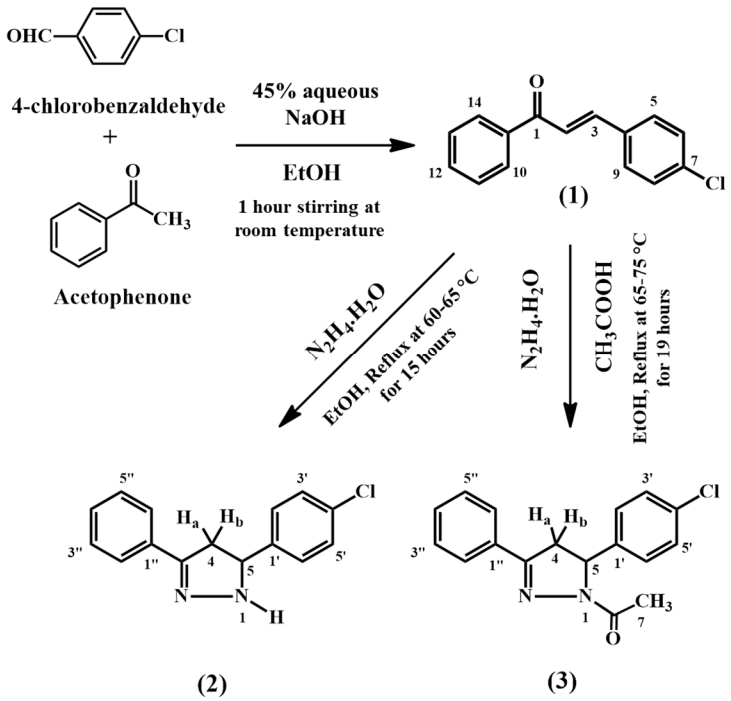

Figure 1. Illustration of reaction scheme of compounds 1-3.

Preparation of 1-(5-(4-chlorophenyl)-3-phenyl-4,5-dihydropyrazol-1-yl) ethanone (3). In this experiment, 1.21 g of compound 1 and 0.25 g (0.25 ml) of $N_2H_4 \cdot H_2O$ were dissolved in 70 ml of ethanol, along with 15 ml of acetic acid, using a beaker containing 0.005 mol of each reactant. After thorough

mixing, the reaction mixture was refluxed at 65-75°C for 19 hrs, with progress monitored hourly by thin-layer chromatography (TLC). Upon completion, the mixture was cooled in an ice-water bath, which led to the formation of a solid precipitate. The crude product was purified by recrystallization from ethanol to afford the pure acetyl pyrazole derivative. The purified compound was then dried under reduced pressure and characterized using melting point determination, UV, IR and ^{1}H NMR spectroscopy to confirm its structure and purity.[21,22]

Yield: 58%; Appearance: Brownish solid; mp: 122-125°C IR (cm^{-1}): 3052 (aromatic C–H stretching), 1733 (C=O stretching), 1589 (C=N stretching), 1147 (C–N stretching), 834 (C–Cl stretching). ^{1}H NMR (400 MHz, $CDCl_3$): δ 2.44 (3H, br s, 7-$COCH_3$), 3.13 (1H, dd, *J* = 12.8, 4.8 Hz, H-4a), 3.82 (1H, dd, *J* = 12, 5.6 Hz, H-4b), 5.56 (1H, dd, *J* = 10.8, 7.2 Hz, H-5), 7.20–7.78 (9H, m, Ar-H).

Cell culture viability assay. The growth-inhibitory effect of the synthesized compounds on cancer cells was evaluated using HeLa cells, a well-characterized human cervical cancer cell line known for its rapid proliferation and frequent use in cancer research. Cells were maintained in Dulbecco's Modified Eagle Medium (DMEM) supplemented with 10% fetal bovine serum (FBS) as a nutrient source, 1% penicillin–streptomycin (1:1) and 0.2% gentamycin to maintain sterility. Four milligrams of each test compound were dissolved in 4 ml of DMSO (5% in H_2O), resulting in a final concentration of 1 mg/ml. HeLa cells (2.0×10^4 cells per 100 µl) were seeded into 48-well plates and incubated overnight at 37°C in a 5% CO_2 atmosphere to maintain physiological pH. Following seeding, 50 µl of the prepared compound solution was added to each well. The plates were further incubated under the same conditions for 24 hrs. Cytotoxic effects were evaluated by observing changes in cell morphology and proliferation using an inverted light microscope. Cell viability was quantified by comparing treated wells with untreated control wells, providing a measure of the compounds' inhibitory effect on HeLa cell growth. The data were used to assess the potential of the synthesized compounds as candidate molecules for antiproliferative drug development.[12]

DPPH (1,1-diphenyl-2-picrylhydrazyl) free radical scavenging assay: The antioxidant potential of the synthesized compounds was evaluated using the DPPH assay, a widely used method that measures the ability of a compound to scavenge free radicals. This method provides a simple, rapid and reliable approach for assessing antioxidant activity of both chemical and biological compounds.[23] In this study, a stable DPPH free radical was employed. Test compound solutions were prepared in methanol at serially diluted concentrations ranging from 100 to 6.125 µg/ml. An aliquot of 1.0 ml of each solution was mixed with 1.5 ml of methanolic DPPH solution. Baseline absorbance was measured using methanol as a blank. The reaction mixtures were incubated in the dark for 30-60 min, and the absorbance was subsequently recorded at 517 nm. The absorbance of the DPPH solution alone was also measured to serve as a reference. The percentage of radical scavenging activity was calculated, and the 50% inhibitory concentration (IC_{50}) of each compound was determined by plotting the percentage inhibition against the compound concentration.[24]

Estimation of total antioxidant capacity. The total antioxidant capacity (TAC) assay is a widely used method for estimating the overall antioxidant potential of a sample by assessing its ability to scavenge free radicals or reactive oxygen species (ROS). This method employs a phosphomolybdenum complex reagent, prepared from sodium phosphate (28 mM), ammonium molybdate (4 mM) and concentrated sulfuric acid (0.6 M). Antioxidants in the sample reduce this complex, resulting in a color change that can be quantified using UV–visible spectrophotometry.[25] In this study, 0.10 ml of each sample, dissolved in methanol at serially diluted concentrations ranging from 200 to 25 µg/ml, was mixed with the reagent in an Eppendorf tube. The mixtures were incubated at 95 °C in a water bath for 1.5 hours. After cooling, the absorbance was measured at 695 nm. Higher absorbance values

corresponded to greater total antioxidant capacity of the sample.

Calculation of drug likeness properties: In Silico pharmacokinetic and drug-likeness prediction: The pharmacokinetic profiles, drug-likeness and physicochemical properties of compounds 1, 2 and 3 were predicted using the web-based tool Swiss ADME (http://www.swissadme.ch/). This program provides a comprehensive assessment of multiple predictive criteria for evaluating the potential of a compound as a drug candidate. For the analysis, the molecular structures or their Simplified Molecular Input Line Entry System (SMILES) notations were submitted.[14] A summary of the evaluated parameters is presented in table 3.

Computer molecular docking analysis: The epidermal growth factor receptor (EGFR) is a transmembrane protein that plays a key role in regulating cell survival, proliferation, and differentiation. Dysregulation of EGFR signaling, through overexpression or mutation, can lead to uncontrolled cellular proliferation and tumorigenesis, making EGFR a critical therapeutic target in cancers such as non-small cell lung cancer, head and neck cancer and colorectal cancer. Several EGFR inhibitors containing pyrazole moieties have been reported previously.[26]

In this study, compounds 1-3, along with the standard EGFR inhibitor erlotinib, were subjected to molecular docking analysis. Three-dimensional (3D) conformers of the compounds in SDF format were retrieved from the PubChem database (https://pubchem.ncbi.nlm.nih.gov/) and drawn using Chem Draw 12.0 software.[27] The crystal structure of EGFR (PDB ID: 1M17) was obtained from the RCSB Protein Data Bank (https://www.rcsb.org/) with a resolution of 2.60 Å.[28] PyMOL version 2.5.2 (Schrödinger, LLC) was used to remove water molecules, ligands, extraneous atoms and surplus protein chains to isolate the receptor-binding domain (RBD) for docking.[29] The prepared protein was saved in PDB format for docking studies.[30] Molecular docking of the synthesized compounds with EGFR was performed using the open-source PyRx software. Binding affinities (kcal/mol), noncovalent interactions and 2D/3D representations of the protein-ligand complexes were analyzed and visualized using BIOVIA Discovery Studio software.[12]

RESULTS AND DISCUSSION

Compound 1 manifested as a yellowish solid and exhibited a yellowish spot upon screening via TLC on silica gel PF_{254}, after treatment with vanillin-sulfuric acid and heating at 80 to 90°C for 5 to 7 min. It was soluble in several organic solvents, including ethanol, ethyl acetate, chloroform and methanol.

The infrared data of compound 1 exhibited distinctive peaks at the following frequencies (cm^{-1}): 3058 (unsaturated C=C–H stretching), 1658 (α,β-unsaturated C=O stretching), 1589 (C=C stretching), 1565 and 1486 (C=C stretching of the aromatic ring), 1402-1446 (saturated C-C stretching), 1214 (aromatic C–C or C–H in-plane bending vibration), and 819 (saturated C-Cl stretching). The ^{1}H NMR spectra (600 MHz, $CDCl_3$) of compound 1 displayed a multiplet at δ 7.39, commensuration to two aromatic protons (H-6 and H-8). Additionally, two multiplets were seen at δ 7.50 and 7.57, corresponding to the aromatic protons with intensities H-2, H-11, H-13 and H-5, H-9, H-12, respectively. Two more deshielded aromatic proton resonances appeared as multiplet at δ 8.01 (H-10 and H-14) attributable to the nearby electronegative keto group at C-1. A doublet at δ 7.76 with a *J* value of 15.6 Hz suggests the presence of H-3 in an *E* alkene. Comparison of the IR and ^{1}H NMR data with previously reported literature[17–19] confirmed the identity of Compound 1 as the chalcone (*E*)-3-(4-chlorophenyl)-1-phenylprop-2-en-1-one.

Compound 2 was obtained as a light orange solid. TLC analysis on silica gel PF_{254} revealed a dark spot under UV light and a yellowish spot after treatment with vanillin-sulfuric acid, followed by heating at 85-95°C for 5-10 minutes. The compound was soluble in ethanol, ethyl acetate, chloroform and methanol. The infrared (IR) spectrum of compound 2

exhibited characteristic absorption bands at the following frequencies (cm^{-1}): 3064 (aromatic C-H stretching), 1589 (C=N stretching of the pyrazoline ring), 1107 (C-N stretching), and 824 (C-Cl stretching). ^1H NMR analysis of compound 2 was performed in $CDCl_3$ at 600 MHz, showing multiplet at δ 3.06, 3.35, and δ 5.31 ppm, corresponding to H-4a, H-4b, and H-5 of the pyrazoline ring, respectively. The –NH (H-1) proton appeared as a broad singlet at δ 7.08. The aromatic protons resonated in the range of δ 7.2–7.6 ppm, integrating for a total of nine protons. Comparison of the obtained NMR data with literature [20,21] values confirmed the structure of compound 2 as 5-(4-chlorophenyl)-3-phenyl-4,5-dihydro-1*H*-pyrazole.

Compound 3 was obtained as a brownish solid. TLC analysis on silica gel PF_{254} revealed a dark spot under UV light and a yellow spot after treatment with vanillin–sulfuric acid, followed by heating at 90-95°C for 8-12 minutes. The compound was soluble in chloroform, ethanol, methanol and ethyl acetate. The infrared (IR) data for compound 3 exhibited characteristic absorption bands at the following frequencies (cm^{-1}): 3052 (aromatic C-H stretching), 1733 (C=O stretching of the acetyl group), 1589 (C=N stretching of the pyrazoline ring), 1147 (C-N stretching) and 834 (C-Cl stretching). ^1H NMR analysis of compound 3 in $CDCl_3$, at 400 MHz, showed double doublets at δ 3.13, 3.82, and δ 5.56 ppm, corresponding to H-4a, H-4b, and H-5 of the pyrazoline ring, respectively, within the pyrazoline ring. The acetyl methyl group ($–COCH_3$) appeared as a broad singlet at δ 2.44 ppm. The aromatic protons resonated in the range δ 7.20–7.78 ppm, integrating for a total of 9 protons. Comparison of the obtained NMR data with reported literature[21,22] values confirmed the structure of compound 3 as 1-(5-(4-chlorophenyl)-3-phenyl-4,5-dihydropyrazol-1-yl) ethanone.

In biomedical research, the HeLa cell line is one of the most widely used human cancer cell lines which was originally derived in 1951 from the cervical carcinoma of Henrietta Lacks. These immortal cells have been extensively utilized to study cancer biology, drug screening and toxicity evaluation. When assessing the anticancer potential of new compounds, cytotoxicity assays using HeLa cells are considered a standard method. These assays evaluate the balance between viable and non-viable cells to determine the cytotoxic effects of tested compounds. In the present study, HeLa cells cultured in growth medium alone exhibited complete survival (100%), and served as the control for normal cell viability. Likewise, cells grown in medium containing blank vehicle demonstrated greater than 95% survival of HeLa cells, confirming that the vehicle itself was non-toxic and well tolerated.

Remarkably, the percentage of surviving HeLa cells decreased drastically to below 5% upon treatment with all synthesized compounds (1-3) indicating strong cytotoxic activity of these test samples. All experimental data were obtained using the cell counting method with a hemocytometer under an inverted phase-contrast microscope, ensuring precise and reproducible results. The cytotoxic responses elicited by compounds 1-3 are comprehensively summarized in table 1.

Table 1. Antiproliferative effect of samples 1-3 using cancerous HeLa cells.

Compound	Survival of cells	Outcome
Media	100%	No cytotoxicity
Media and vehicle	Greater than 95%	No cytotoxicity
1	Less than 5%	Cytotoxicity
2	Less than 5%	Cytotoxicity
3	Less than 5%	Cytotoxicity

In drug discovery programs, assessing the antioxidant capabilities of novel compounds is a crucial step, and the 2,2-diphenyl-1-picrylhydrazyl (DPPH) radical scavenging assay is among the most widely used and cost-effective methods for this purpose. The principle of this assay is based on the ability of test compounds to donate electrons or hydrogen atoms to neutralize the stable, purple-colored DPPH free radical, leading to a decrease in absorbance. The extent of this decrease directly reflects the free radical scavenging ability of the tested compounds. Owing to its simplicity,

reproducibility and sensitivity, the DPPH assay is extensively applied for the preliminary screening of potential antioxidant agents in pharmacological research. In the present study, all tested compounds exhibited a dose-dependent reduction in DPPH radical absorbance, confirming their ability to neutralize free radicals. Among them, compound 1 showed the strongest antioxidant effect, with an IC_{50} value of 35.2 µg/ml, indicating higher scavenging activity compared to the other derivatives. These observations are consistent with previous findings[24], which suggest that compounds capable of donating hydrogen atoms or electrons can effectively reduce oxidative stress markers.

Similarly, in the total antioxidant capacity (TAC) assay, which measures the combined antioxidants effect of all constituents in a sample, compound 1 again demonstrated the highest activity, consistent with the DPPH results. As presented in table 2 and figure 2, the order of antioxidant activity in both assays was: compound 1 > compound 2 > compound 3. This consistency between the two assay systems highlights the potent antioxidant potential of compound 1 and underscores its promise as a lead candidate for further pharmacological investigation targeting oxidative stress-related disorders.

Table 2. IC_{50} value of free radical sequestering activity of all three compounds (1-3).

Sample	IC_{50} ± SD (µg/ml)
Butylated hydroxy toluene (BHT)	10.7 ± 0.03
1	35.2 ± 0.15
2	40 ± 0.40
3	53.3 ± 0.42

Expression of outcomes are as average ± standard deviation (SD), where sampling size is n=3.

The total antioxidant capacity (TAC) assay is a widely used and well-established method used to evaluate the overall reducing power of bioactive compounds. In this test, antioxidants present in the sample act as reducing agents when mixed with an acidic medium containing molybdate ions, this reaction leading to the formation of a green phosphomolybdenum complex. The intensity of this complex, measured spectrophotometrically, is directly proportional to the concentration and potency of antioxidants within the sample. The deeper the color, the greater the concentration and strength of antioxidants present in the sample. In this present study (Figure 2), compounds 1-3 displayed a clear dose-dependent increase in antioxidant activity, with compound 1 demonstrating the strongest reducing ability, followed by compounds 2 and 3. These results closely corresponded those obtained from the DPPH assay, further confirming the antioxidant potential of the synthesized molecules. The consistency observed between both assays indicates that these compounds can effectively neutralize free radicals and participate in redox reactions that mitigate oxidative intermediates.[25] Overall, these findings suggest that compounds 1-3 possess promising antioxidant activity with potential therapeutic relevance. Considering the critical role of oxidative stress in the pathogenesis of various chronic and degenerative diseases -such as neurodegenerative disorders, diabetes and cardiovascular conditions—the tested compounds may serve as valuable leads for the development of antioxidant-based pharmacological interventions. Considering the critical role of oxidative stress in the pathogenesis of various chronic and degenerative diseases—such as neurodegenerative disorders, diabetes and cardiovascular conditions—these compounds may serve as valuable leads for the development of antioxidant-based pharmacological interventions.

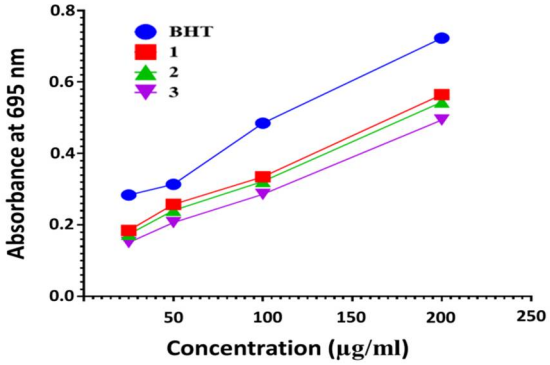

Figure 2. Comparative graph of total antioxidant capacity of samples 1-3 and standard, BHT.

Utilizing the SwissADME web-based tool (http://www.swissadme.ch/), the pharmacokinetic, physicochemical and drug-likeness status of compounds 1-3 was assessed[14] (Table 3). All three compounds fell within a narrow size range and exhibited moderate lipophilicity, features typically associated with favorable oral bioavailability. Their very low topological polar surface area (TPSA) values and limited hydrogen-bonding capacity suggested strong potential for passive membrane permeation. Predicted gastro-intestinal absorption was high for each molecule, further supporting their suitability for oral administration. Blood–brain barrier (BBB) permeability was also predicted to be positive across the series, indicating the potential for central nervous system (CNS) penetration. None of the compounds was predicted to be a P-glycoprotein substrate, reducing the likelihood of efflux-related absorption limits. The series demonstrated consistent inhibition of CYP-2C9, CYP-1A2 and CYP-2C19 isoenzymes, warranting caution for possible metabolic drug–drug interactions. In contrast, CYP-2D6 and CYP-3A4 inhibition were not broadly predicted, suggesting a lower risk of widespread metabolic interference. All compounds complied with Lipinski's rule of five and other standard drug-likeness criteria, each exhibiting a bioavailability score of 0.55. Overall, these findings indicate that the synthesized molecules possess characteristics consistent with orally bioavailable and CNS-active agents; however, further optimization should focus on improving selectivity against specific CYP isoforms and fine-tuning molecular polarity.

Table 3. *In silico* estimation of the drug-likeness characteristics of compounds 1-3.

Parameters	1	2	3
A) Physicochemical properties			
Formula	$C_{15}H_{11}ClO$	$C_{15}H_{13}ClN_2$	$C_{17}H_{15}ClN_2O$
Molecular weight (g/mol)	242.70	256.73	298.77
Heavy atoms (count)	17	18	21
Aromatic heavy atoms	12	12	12
Molecular volume	215.39	227.44	263.36
Molar refractivity	71.76	82.13	92.04
XLOGP	3.71	3.95	3.46
MLOGP	3.96	3.53	3.33
TPSA (Å²)	17.07	24.39	32.67
Donors of H-bond	0	1	0
Acceptors of H-bond	1	1	2
Rotatable bonds (RB)	3	2	3
B) Pharmacokinetics			
Blood–brain barrier permeation	+	+	+
GI absorption	Excessive	Excessive	Excessive
P-glycoprotein substrate	-	-	-
Inhibition of CYP-1A2	+	+	-
Inhibition of CYP-2C9	+	+	+
Inhibition of CYP-2C19	+	+	+
Inhibition of CYP-2D6	-	+	-
Inhibition of CYP-3A4	-	-	-
C) Drug likeliness filters			
Lipinski rule	+, 0 violation	+, 0 violation	+, 0 violation
Veber rule	+	+	+
Muegge rule	-, 1 violation	+	+
Bioavailability score	0.55	0.55	0.55

Here, TPSA, Topological polar surface area; CYP., Cytochrome; +, Positive outcome; -, Negative outcome; XLOGP, Octanol by water partition coefficient (atom-additive method); MLOGP, Moriguchi concept of octanol-water partition coefficient; Filter criteria, Lipinski: $MLOGP \leq 4.15$; $MW \leq 500$; $HBD \leq 5$; $HBA \leq 10$; Muegge: $HBD \leq 5$; $RB \leq 15$; $-2 \leq XLOGP \leq 5$; $200 \leq MW \leq 600$; HBA

≤ 10; TPSA ≤ 157; Ring number ≤ 7; Number of carbons > 4; Heteroatom number > 1; Veber: Rotatable bonds ≤ 10; TPSA ≤ 140 Å^2.

The molecular docking study (Table 4 and Figure 3) revealed that all three compounds bound effectively to the target protein, exhibiting stronger affinities than the reference inhibitor, erlotinib. Among them, compound 3 showed the most stable binding, with a docking energy of –7.8 kcal/mol, which was lower than that of Erlotinib's (–7.0 kcal/mol). Compounds 1 and 2 also displayed favorable binding affinities (–7.5 kcal/mol), suggesting comparable or potentially superior activity relative to the standard. The ligands consistently interacted with key amino acid residues such as *Ala* 48, *Lys* 50, *Leu* 93, *Met* 71 and *Val* 31, which are critical for stabilizing the ligand–protein complex.

Table 4. The binding affinities of drugs 1 through 3, as well as standard drug, erlotinib.

Samples	Bond energy (Kcal/mol)	Binding interactions (three letter code of AA residue)
Erlotinib (Standard inhibitor)	-7.0	*Ala* 48, *Lys* 50, *Leu* 93, *Leu* 23, *Met* 71, *Asp* 160, *Val* 31
1	-7.5	*Ala* 48, *Lys* 50, *Leu* 23, *Leu* 93, *Leu* 149, *Thr* 159, *Met* 71
2	-7.5	*Ala* 48, *Lys* 50, *Leu* 23, *Leu* 93, *Val* 31, *Met* 71
3	-7.8	*Ala* 48, *Lys* 50, *Leu* 93, *Val* 31, *Met* 71

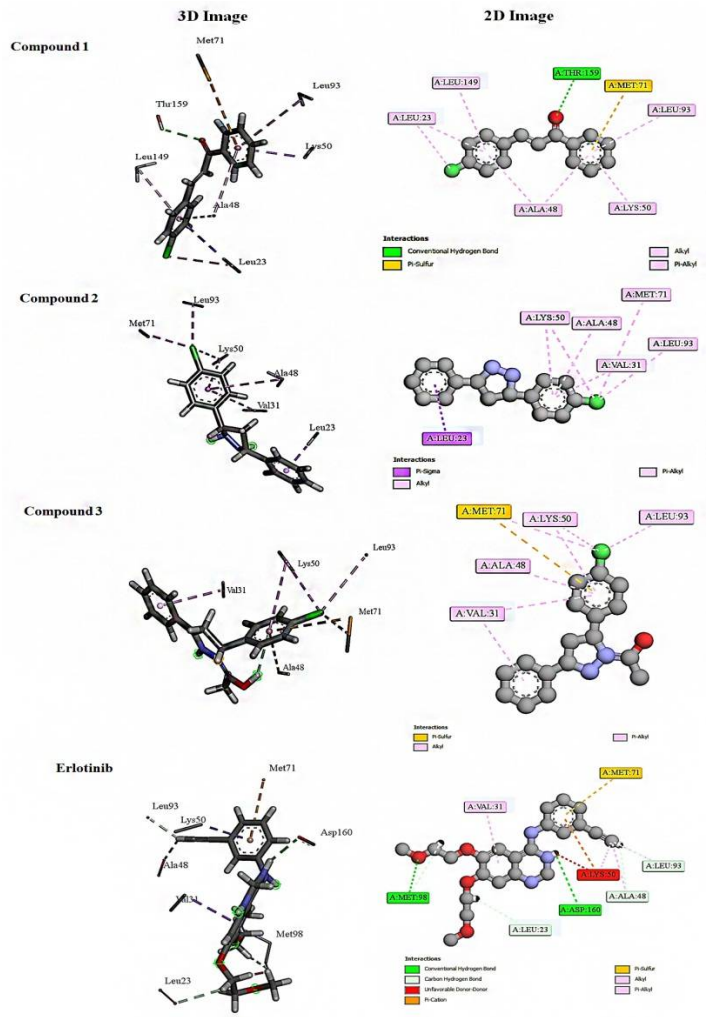

Figure 3. Illustrative 3D and 2D docking pictures of samples **1 - 3** as well as erlotinib, an EGRF inhibitor, respectively.

Hydrophobic contacts, complemented by hydrogen-bonding interactions, further reinforced the binding stability within the active site. The recurring involvement of *Ala* 48 and *Lys* 50 across all ligands underscored their importance in anchoring the molecules within the binding pocket. Compared with erlotinib, the test compounds established a broader interaction network with the active-site residues, which may contribute to enhanced inhibitory potential. Overall, these findings suggest that compounds 1-3, particularly compound 3, represent promising lead candidates for further structural optimization and biological validation.

CONCLUSION

The present investigation successfully synthesized and characterized three compounds, (*E*)-3-(4-chlorophenyl)-1-phenylprop-2-en-1-one (1), 5-(4-chlorophenyl)-3-phenyl-4,5-dihydro-1*H*-pyrazole (2), and 1-(5-(4-chlorophenyl) -3-phenyl-4,5-dihydropyrazol-1-yl) ethanone (3). Structural elucidation was confirmed through FT-IR and NMR spectroscopy. All three compounds exhibited strong antiproliferative effects against HeLa cells, reducing cell survival rates below 5%, thereby highlighting their significant anticancer potential. Antioxidant assays revealed that compound 1 demonstrated the highest radical scavenging capacity, followed by compounds 2 and 3, underscoring the superior antioxidant potential of the chalcone scaffold. Molecular docking studies against the epidermal growth factor receptor (EGFR) indicated favorable binding affinities for all three compounds, with compound 3 showing the strongest interaction (-7.8 kcal/mol), surpassing that of the reference inhibitor erlotinib. SwissADME predictions suggested good gastrointestinal absorption, blood–brain barrier permeability and acceptable bioavailability scores for the entire series. However, compounds 1 and 2 showed possible interactions with CYP isoenzymes and minor lead-likeness violations, whereas compound 3 satisfied most drug-likeness criteria. Despite these promising findings, certain limitations persist. The cytotoxic mechanism remains to be fully elucidated. *In vitro* evaluation was confined to HeLa cells without comparison to other cancer or normal cell lines, and experimental ADMET validation was not performed. Future studies should focus on structural refinement—particularly of compounds 1 and 2—to mitigate CYP inhibition while maintaining biological activity. This study presents, for the first time, the biological and computational evaluation of these compounds. Overall, the chalcone–pyrazole derivatives showed significant antioxidant and anticancer potential, highlighting the need for further pharmacokinetic and biological investigations.

ACKNOWLEDGEMENT

This research was made possible by the funding that was granted to MSR by the University Grants Commission of Bangladesh for the fiscal year 2021-2022.

REFERENCES

1. Mahapatra, A., Prasad, T. and Sharma, T. 2021. Pyrimidine: a review on anticancer activity with key emphasis on SAR. *Futur. J. Pharm. Sci.* **7**, 123-125.
2. Ardiansah, B. 2019. Chalcones bearing N, O and S-heterocycles: recent notes on their biological significances. *J. Appl. Pharm. Sci.* **9**, 1-10.
3. Mezgebe, K., Melaku, Y. and Mulugeta, E. 2023. Synthesis and pharmacological activities of chalcone and its derivatives bearing N-heterocyclic scaffolds: a review. *ACS omega*, **8**, 19194-19211.
4. Kumar, V. and Jayaroopa, R. 2013. Pyrazole containing natural products: synthetic preview and pharmacological significance. *Natur. Prod. Res.* **27**, 487-496.
5. Albratty, M. and Alhazmi, H.A. 2022. Novel pyridine, and pyrimidine derivatives as promising anticancer agents: a review. *Arab. J. Chem.* **15**, 103846.
6. Shaik, A.B., Bhandare, R.R., Nissankararao, S., Edis, Z., Tangirala, N.R., Shahanaaz, S. and Rahman, M.M. 2020. Design, facile synthesis and characterization of dichloro substituted chalcones and dihydropyrazole derivatives for their antifungal, antitubercular and antiproliferative activities. *Molecules* **25**, 3188-3193.
7. Fearon, I.M. and Faux, S.P. 2009. Oxidative stress, and cardiovascular disease: novel tools give free radical insight. *J. Mol. Cell. Cardiol.* **47**, 372-381.

8. Tamura, H., Takasaki, A., Miwa, I., Taniguchi, K., Maekawa, R., Asada, H., Taketani, T., Matsuoka, A., Yamagata, Y., Shimamura, K., Morioka, H., Ishikawa, H., Reiter, R.J. and Sugino, N. 2008. Oxidative stress impairs oocyte quality and melatonin protects oocytes from free radical damage and improves fertilization rate. *J. Pineal Res.* **44**, 280-287.
9. Victor, V.M., Rocha, M., Sola, E., Banuls, C., Garcia-Malpartida, K. and Hernandez-Mijares, A. 2009. Mitochondria-targeted antioxidant peptides. *Curr. Pharm. Des.* **15**, 2988-3002.
10. Ali, M.S., Rani, S.H. and Kumar, S. 2017. Pyrazole-based derivatives as potent antioxidants: a comprehensive review. *Eur. J. Med. Chem.* **141,** 1-15.
11. Rani, J., Saini, M., Kumar, S. and Verma, P.K. 2017. Design, synthesis and biological potentials of novel tetrahydroimidazo [1,2-a] pyrimidine derivatives. *Chem. Cent. J.* **11**, 16-22.
12. Dallakyan, S. and Olson, A.J. 2015. Small-molecule library screening by docking with PyRx. *Methods Protoc.* **243**, 250-255.
13. Yu, X. (2022). Global reactivity descriptors in the design of chalcone derivatives. *J. Mol. Mod.* **28**, 1-9.
14. Daina, A., Michielin, O. and Zoete, V. 2017. SwissADME: a free web tool to evaluate pharmacokinetics, drug-likeness and medicinal chemistry friendliness of small molecules. *Sci. Rep.* **7,** 42717.
15. Elkanzi, N.A.A. 2022. Synthesis of chalcone derivatives and their biological activities. *ACS Omega*, **7**, 4567-4575.
16. Ganji, N.R., Shabanzadeh, M., Moghaddam, P.S. and Ganji, S.R. 2023. Cytotoxic effects of ibuprofen on cervical cancer HeLa cells through induction of nitric oxide synthase 2 (iNOS) gene expression. *J. Biol. Sci.* **6,** 169-177.
17. Ghoshir, U., Kande, S.R., Muley, G.G. and Gambhire, A.B. 2019. Synthesis and characterization of co-doped fly ash catalyst for chalcone synthesis. *Asian J. Chem.* **31,** 2165-2172.
18. Mameda, N., Peraka, S., Kodumuri, S., Chevella, D., Banothu, R., Amrutham, V. and Nama, N. 2016. Synthesis of α, β - unsaturated ketones from alkynes, and aldehydes over H_β zeolite under solvent-free conditions. *RSC Adv.* **6**, 58137-58141.
19. Wong, Q.A., Quah, C.K., Wong, X.A., Maidur, S.R., Kwong, H.C., Win, Y.F., Patil, P.S. and Gummagol, N.B. 2022. Structure–property relationship of three 2-chloro-4-fluoro chalcone derivatives: a comprehensive study on linear and non-linear optical properties, structural characterizations and density functional theory. *J. Mol. Struct.* **1267,** 133584.
20. Ranganathan, K., Suresh, R., Vanangamudi, G., Thirumurthy, K., Mayavel, P. and Thirunarayanan, G. 2014. $SOCl_2$ catalyzed cyclization of chalcones: synthesis and spectral studies of some bio-potent ^1H pyrazoles. *Bull. Chem. Soc. Ethiop.* **28**, 271-288.
21. Safaei-Ghomi, J., Bamoniri, A. and Soltanian-Telkabadi, M. 2006. A modified and convenient method for the preparation of N-phenyl pyrazoline derivatives. *J. Heterocycl. Chem.* **42**, 892-896.
22. Hamad Elgazwy, A.S.S., Soliman, D.S., Atta-Allah, S.R. and Diaa A.I. 2012. Three-dimensional quantitative structure activity relationship (QSAR) of cytotoxic active 3,5-diaryl-4,5-dihydropyrazole analogues: a comparative molecular field analysis (CoMFA) revisited study. *Chem. Cent. J.* **6**, 50.
23. Sökmen, M. and Akram Khan, M. 2016. The antioxidant activity of some curcuminoids and chalcones. *Inflammopharmacology* **24**, 81-86.
24. Brand-Williams, W., Cuvelier, M. E. and Berset, C. 1995. Use of a free radical method to evaluate antioxidant activity. *Lebensm. Wiss. Technol.* **28**, 25-30.
25. Prieto, P., Pineda, M. and Aguilar, M. 1999. Spectrophotometric quantitation of antioxidant capacity through the formation of a phosphor-molybdenum complex: specific application to the determination of vitamin E. *Anal. Biochem.* **269**, 337-341.
26. Kurban, B., Sağlık, B.N., Osmaniye, D., Levent, S., Özkay, Y. and Kaplancıklı, Z.A. 2023. Synthesis, and anticancer activities of pyrazole–thiadiazole-based EGFR inhibitors. *ACS Omega* **8,** 31500-31509.
27. Kim, S., Chen, J., Cheng, T., Gindulyte, A., He, J., He, S., Li, Q., Shoemaker, B.A., Thiessen, P.A., Yu, B., Zaslavsky, L., Zhang, J. and Bolton, E.E. 2019. PubChem 2019 update: improved access to chemical data. *Nucleic Acids Res.* **47,** D1102-D1109.
28. Stamos, J., Sliwkowski, M.X. and Eigenbrot, C. 2002. Structure of the epidermal growth factor receptor kinase domain alone and in complex with a 4-anilinoquinazoline inhibitor. *J. Biol. Chem.* **277,** 46265-46272.
29. Lill, M.A. and Danielson, M.L. 2011. Computer-aided drug design platform using PyMOL. *J. Comput. Aided Mol. Des.* **25,** 1-5.
30. Morris, G.M. and Lim-Wilby, M. 2008. Molecular docking. *J. Mol. Model* **443,** 365-382.